

Electrochemical Response and Impedimetric Behaviour of Dopamine and Epinephrine at Platinum Electrode Modified with Carbon Nanotubes-Gold Nanocomposite

Abolanle S. Adekunle^{1,2}, Joseph G. Ayenimo^{2,3,*}, Xi-Ya Fang⁴, Winston O. Doherty^{2,3},
Omotayo A. Arotiba¹, Bhekhe B. Mamba¹

¹Department of Chemical Technology, University of Johannesburg, P.O. Box 17011, Doornfontein, 2028, South Africa

²Department of Chemistry, Obafemi Awolowo University Ile-Ife, Nigeria.

³School of Applied Sciences & Engineering, Monash University, Gippsland Campus, Churchill 3842, Victoria, Australia.

⁴Monash Centre for Electron Microscopy, Monash University, Clayton campus, Victoria 3800, Australia.

*E-mail: Ayenimo71@yahoo.com

Received: 15 April 2011 / Accepted: 30 May 2011 / Published: 1 July 2011

A Platinum (Pt) electrode was modified with gold and gold oxide nanoparticles electrodeposited on multi-walled carbon nanotubes. The modified electrodes were characterised with techniques such as Transmission Emission Microscopy (TEM), Scanning Electron Microscopy (SEM), and Energy Dispersive X-ray Spectroscopy (EDX). The electrochemical properties were investigated using cyclic voltammetry, square wave voltammetry and electrochemical impedance spectroscopy. The electrodes were used as analytical probes towards the detection of dopamine (DA) and epinephrine (EP). Results showed that Pt-MWCNT-Au electrode gave the best dopamine and epinephrine current response at lower charge transfer resistance R_{ct} values of 9.1 and 9.4 Ωcm^2 in DA and EP respectively compared with other electrodes. The electrooxidation of the analyte involved adsorbed intermediates with adsorptive capacitance (C_{ads}) and Tafel values of, 331.6 μFcm^{-2} , 136.4 mVdec^{-1} in DA; and 225.2 μFcm^{-2} , 162.8 mVdec^{-1} in EP. The limit of detection were 78 ± 6.5 nM and 350 ± 28.4 nM while the catalytic rate constant (K) were (13.8 ± 2.4) and $(18.9\pm 4.2) \times 10^8$ $\text{cm}^3 \text{mol}^{-1} \text{s}^{-1}$ for DA and EP respectively on the electrode. The limit of detection is favourable for DA detection in biological system where DA exists in μM concentration. The electrode was easy to prepare and was also electrochemically stable such that it could be used for the detection of DA and EP in the presence of interfering species such as ascorbic acid (AA).

Keywords: Multi-walled carbon nanotubes, gold nanoparticles, platinum electrode, impedance spectroscopy, biological analytes, interferences.

1. INTRODUCTION

Dopamine (DA) is an important neurotransmitter in the mammalian central nervous, hormonal and renal system [1]. It can cause Parkinson's disease (when in low amount) and other similar diseases [2,3]. Epinephrine, (EP) on the other hand belongs to the group of substances known as catecholamine neurotransmitters which include norepinephrine and dopamine [4,5]. They are mainly important for message transfer in the mammalian central nervous system (CNS). Changes in concentration of epinephrine in the body can result in many diseases such as Alzheimer's disease and aging effect [6]; hence its detection and quantification under physiological pH conditions is of great interest to researchers. Dopamine and epinephrine exist in the CNS and body fluids as organic cations and always coexists with ascorbic acid in biological systems [4,5]. Therefore, various analytical methods to detect these analytes have been developed in the past. Some examples of these methods are the liquid chromatography, mass spectrometry [7], gas chromatography methods [8], and capillary electrophoresis mass spectrometry method [9]. These methods require several derivatization procedures which are time consuming and very expensive. Simultaneous detection of DA or EP in the presence of ascorbic acid (AA) and uric acid (UA) is a critical challenge not only in the field of biomedical chemistry and neurochemistry but also for diagnostic and pathological research. It is known that with a bare electrode the oxidation peaks of DA and AA are at nearly same potential, which results in the overlapped voltammetric responses making their discrimination very difficult [10]. Thus, there is need for the fabrication of sensitive, specific and selective biosensors that would discriminately detect DA and EP in the presence of other interfering species such as ascorbic and uric acids. Electrochemical methods provide a simple, cost effective and quick way of analyzing biologically and environmentally important molecules.

Carbon nanotubes are excellent electrical conducting nanowires with unique properties such as high tensile strength, electrical conductivity, chemical stability and flexibility. Their contribution to the improvement of the electrical properties of some bare electrode such as the glassy carbon [11], graphite [12], carbon fiber [13], gold [14], and platinum (Pt) electrodes [15] have been reported. In the same vein, the use of platinum (Pt) or gold (Au) nanoparticles modified electrode in catalysis is becoming of increased interest owing to their improved performance. A carbon-supported bi-metallic AuPt nanoparticle was reported for electrocatalytic oxidation of methanol [16]. AuPt alloy nanoparticle catalysts were used in the electrocatalytic reduction of oxygen [17]. The determination of DA was carried out using a polymer matrix and gold nanoparticles [18]. Gold nanoparticles immobilized on amine-terminated self-assembled monolayers (SAM) on a polycrystalline Au electrode were successfully used for the selective determination of DA in the presence of an ascorbate species [19]. Other studies involving electrooxidation of DA and EP on gold nanoparticle modified electrodes have been reported [20-23]. There are many reports on DA and EP detection but unfortunately, there are limited reports on the impedimetric behaviour towards DA and EP detection using CNT-Au nanocomposite modified electrode conformation.

In this study, we have for the first time explored the unique potential of a simple, cost effective and easily prepared sensor made from CNT-gold nanoparticles on Pt based electrode for the detection of DA and EP, and their electronic behaviour on the electrode compared with other modified

electrodes using impedimetric studies. The study showed that the detection of these two important biomolecules was possible even at nano molar concentrations. The impedance studies indicated that the analytes behaved similarly with close resistance to charge transfer values. The fabricated sensor can easily detect DA or EP in the presence of interfering compounds such as ascorbic acid (AA) even at a potential broad enough for the simultaneous separation of these molecules from AA.

2. EXPERIMENTAL

2.1. Materials and Reagents

Multi-walled carbon nanotubes were purchased from Aldrich Chemical and were acid treated to introduce carboxylic functional groups (or carboxylated multi-walled carbon nanotubes (CMC)) using a standard procedure [24]. Dopamine-hydrochloride and epinephrine hydrochloride were purchased from Sigma-Aldrich. Other chemicals and reagents were of analytical grade. Ultra pure water of resistivity 18.2 M Ω cm was obtained from a Milli-Q Water System (Millipore Corp., Bedford, MA, USA) and was used throughout the experiment. A phosphate buffer solution (PBS) of pH 7.0 was prepared with appropriate amounts of NaH₂PO₄·2H₂O and Na₂HPO₄·2H₂O, and the pH was adjusted with 0.1 M H₃PO₄ or NaOH. All solutions were purged with pure nitrogen to eliminate oxygen during electrochemical measurements or any form of external oxidation during the experiments.

2.2. Equipment and Procedure

The working electrode, bare platinum (d = 2.0 mm) was purchase from BASi, USA. High resolution scanning electron microscopy (HRSEM) image was obtained using the Zeiss Ultra Plus 55 HRSEM (Germany), while the energy dispersive x-ray spectra (EDX) were obtained from NORAN VANTAGE (USA). The Transmission electron microscopy (TEM) characterisation was performed using a Model JEOL JEM-2100F Field Emission Transmission Electron Microscope. Electrochemical experiments were carried out using an Autolab Potentiostat PGSTAT 302 (Eco Chemie, Utrecht, and The Netherlands) driven by the GPES software version 4.9. Electrochemical impedance spectroscopy (EIS) measurements were performed with an Autolab Frequency Response Analyser (FRA) software between 10 kHz and 0.1 Hz using a 5 mV rms sinusoidal modulation in 5 mM [Fe(CN)₆]⁴⁻/[Fe(CN)₆]³⁻ solution at a fixed potential of 0.2 V. The reference and counter electrodes used were Ag|AgCl in saturated KCl and platinum wire respectively. A bench top pH / ISE ORION meter, model 420A, was used for pH measurements. All solutions were de-aerated by bubbling nitrogen prior to each electrochemical experiment. All experiments were performed at 25 ± 1 °C.

2.3. Electrode modification procedure

Platinum electrode was cleaned by gentle polishing in aqueous slurry of alumina nanopowder, Sigma-Aldrich (grain size <100 nm) on a SiC-emery paper, mirror finished on a Buehler felt pad and was subjected to ultrasonic vibration in absolute ethanol and water successively. Pt-CMC was prepared

by a drop-dry method using 10 μL drop of the CMC solution (0.1 mg CMC in 1 ml DMF). The Pt-CMC electrode was dried in an oven at 50 $^{\circ}\text{C}$ for about 2 min. Gold nanoparticles were electrodeposited on the Pt-CMC electrode from 5.3 mM colloidal gold solutions using chronoamperometric technique at fixed potential of -2.0 V for 5 mins [25,26]. The Pt-CMC-Au electrode obtained was immersed in 20 mls, 0.1 M PBS (pH 7.0) and repetitively scanned (20 scans) between the 1.5 and -0.8 V potential window at a scan rate of 100 mVs^{-1} [26]. The Pt-CMC-AuO electrode obtained was rinsed with distilled water and air-dried. The same procedures were used for the electro-deposition of Au and AuO nanoparticles on glassy carbon plate for SEM pictures morphology changes since it is the available plate that can conveniently fit into the SEM machine.

3. RESULTS AND DISCUSSION

3.1. Comparative SEM, TEM and EDX profile

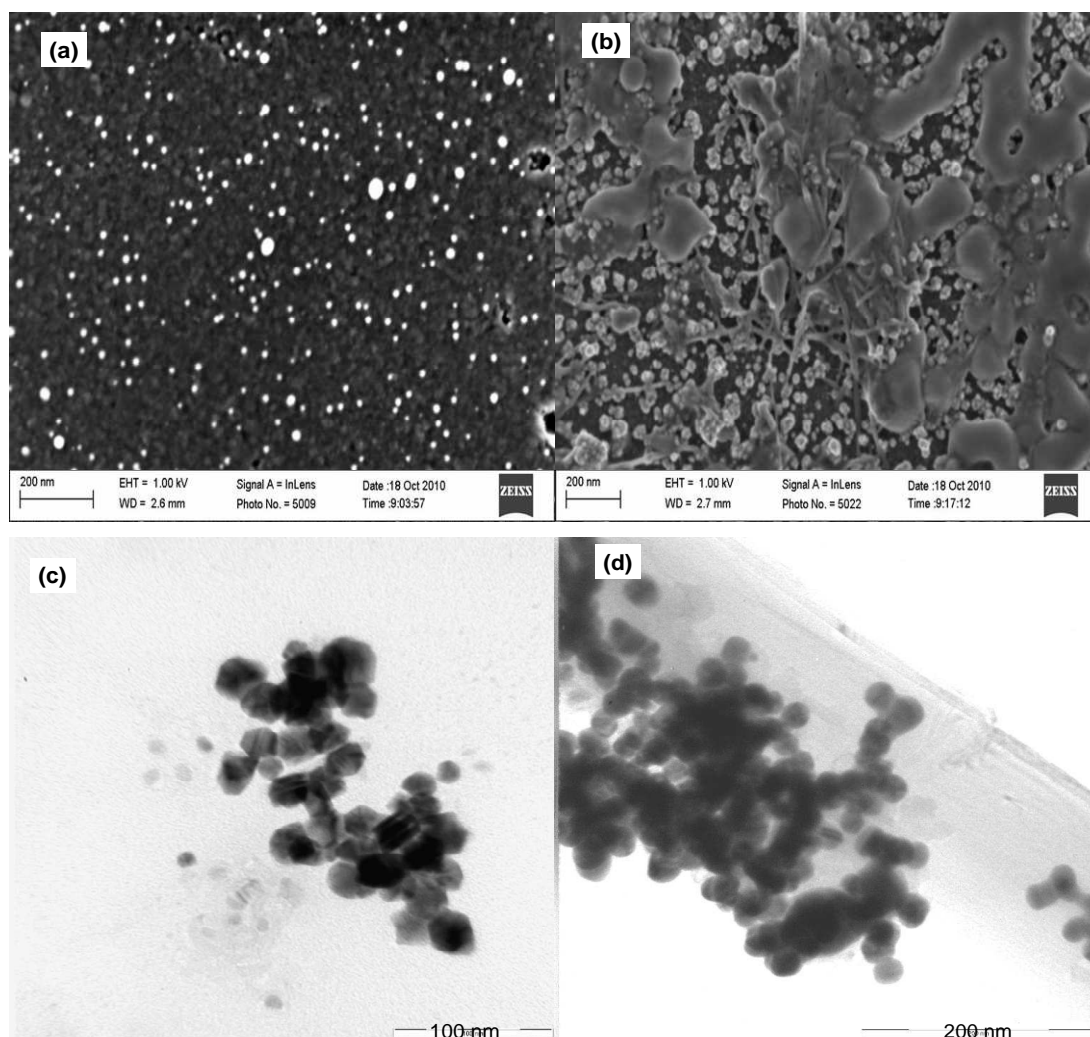


Figure 1. SEM images of (a) Au and (b) CMC-Au nanoparticles. (c) and (d) are their respective TEM images.

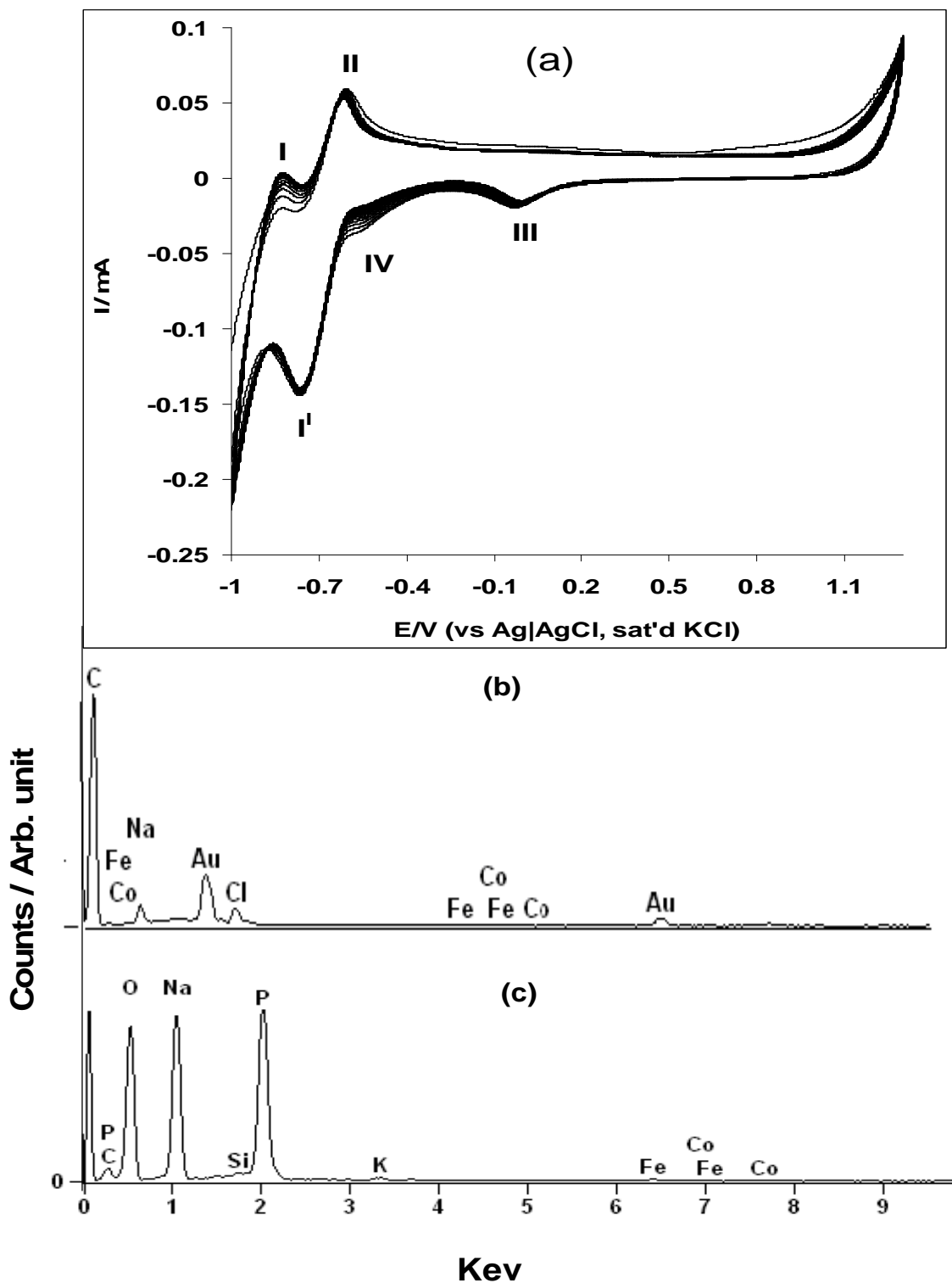


Figure 2. (a) Repetitive cyclic voltammograms (20 scans) of Pt-CMC-Au modified electrode in pH 7.0 PBS, scan rate: 100 mVs⁻¹. (b) EDX profile of the Pt-Au nanoparticles electrode (c) EDX profile of the CMC-Au oxide nanoparticles modified electrode.

Figure 1 presents the SEM images of (a) Au nanoparticles and (b) CMC-Au nanoparticles modified electrodes. There was high dispersion of Au nanoparticles, which is uniformly distributed on the GC plate. TEM images (Fig. 1c and 1d) clearly showed that the Au nanoparticles appeared

amorphous, and distributed along the CMC. This is most likely due to simple electrostatic interaction between the COO^- and the Au^{2+} ions.

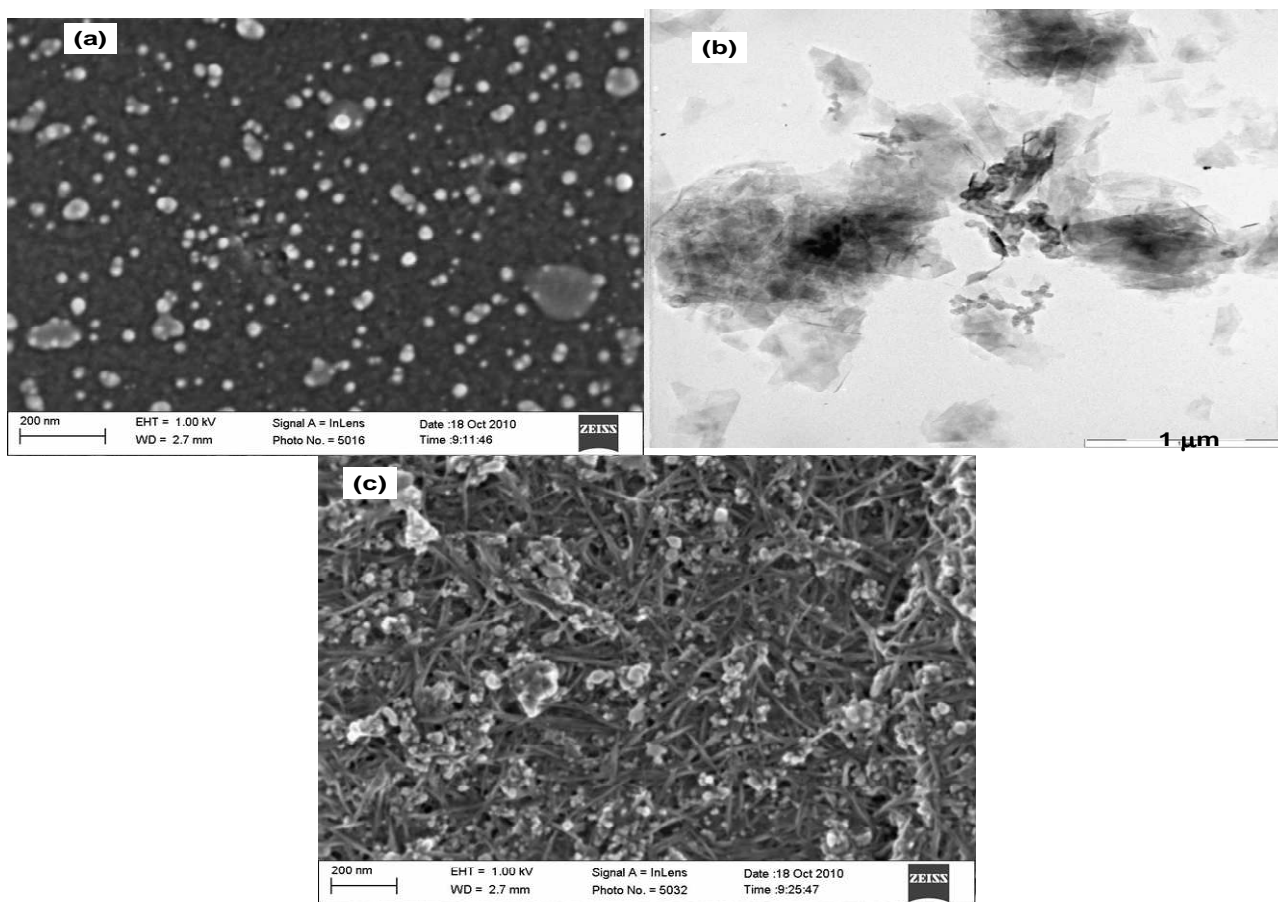


Figure 3. (a) SEM image of Au oxide (b) TEM image of the Au oxide nanoparticles and (c) SEM image CMC-Au oxide nanoparticles.

Repetitive cycling (20 scans, Fig. 2a) of the Pt-CMC-Au electrode in 0.1 M pH 7.0 phosphate buffer solution (PBS) gave the Pt-CMC-AuO modified electrode. The CV showed two redox peaks at -0.82 and -0.61 V corresponding to Pt/Pt^{2+} and $\text{Pt}^{2+}/\text{Pt}^{3+}$ processes at **I** and **II**. The reduction peaks at -0.56 V (**IV**) and -0.77 V (**I'**) correspond to the reduction of $\text{Pt}^{3+}/\text{Pt}^{2+}$ and Pt^{2+}/Pt . The reduction peak at -0.02 V is attributed to the reduction of Au^{2+}/Au (**III**). This peak is dominant over its oxidation peak (not visible) probably because of the very high stability of Au in the oxidation state zero (0). The Au reduction peak is observed at much lower potential on our modified electrode compared with 0.7 V reported on gold nanoparticle modified glassy carbon electrode [23] due to the different pH and reference electrode.

The Au peak in the EDX profile (Fig. 2b) of Pt-CMC-Au modified electrode confirms successful modification of the Pt electrode with Au nanoparticles. Even though the Au peak is not visible in Figure 2c, the prominence of O peak suggests the transformation of the Au to AuO nanoparticles as represented by completely different morphology (see Fig. 3). Infact, the TEM image

of the Pt-AuO electrode (Fig. 3b) clearly indicates a thick, crystalline AuO nanoparticles layers aggregating. The AuO crystalline layers could be responsible for the disappearance of the Au peak in the EDX profile of the AuO modified electrodes since the EDX technique only provides information on few nanometer layers of the modified surface. From the TEM, the particle sizes of the Au and the AuO nanoparticles are in the 10 – 30 and 20 – 60 nm range respectively.

3.2. Electrochemical behaviour of the modified electrodes

Figure 4 presents the current responses (electron transport) of the modified electrodes in 5 mM $[\text{Fe}(\text{CN})_6]^{4-}/[\text{Fe}(\text{CN})_6]^{3-}$ redox probe solution.

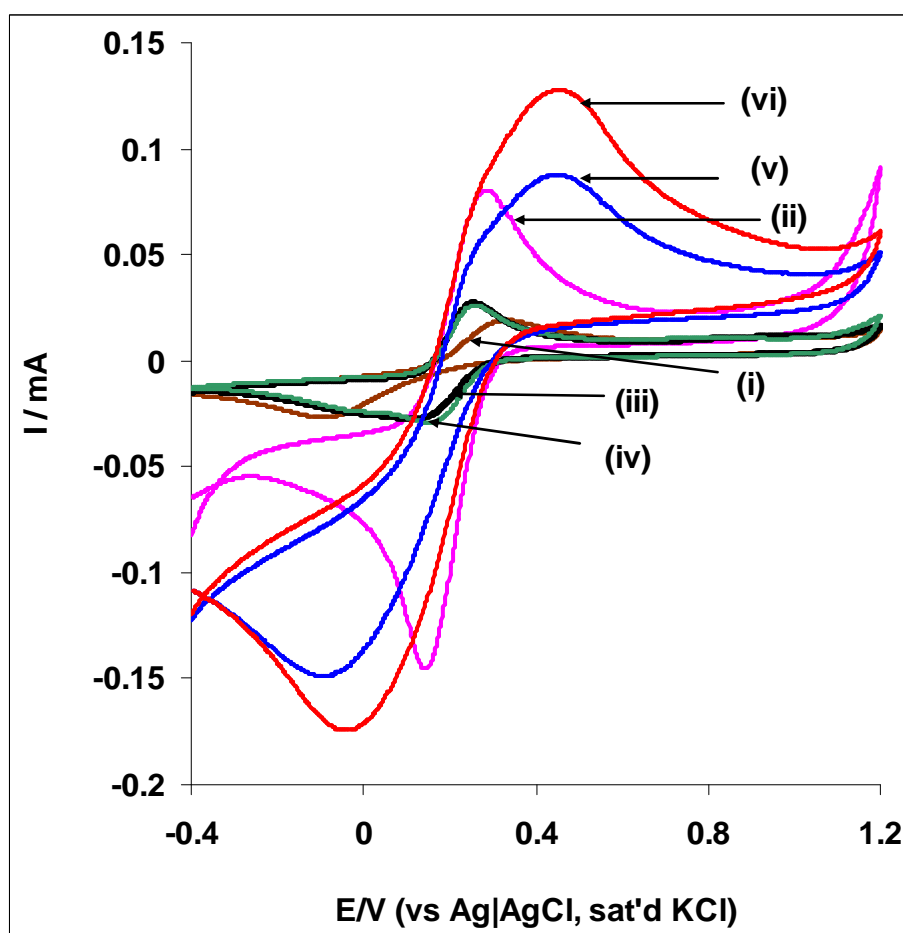


Figure 4. Comparative cyclic voltammetric evolutions of the electrodes in (i) Pt, (ii) Pt-CMC, (iii) Pt-Au, (iv) Pt-AuO, (v) Pt-CMC-Au and (vi) Pt-CMC-AuO in 5 mM $[\text{Fe}(\text{CN})_6]^{4-} / [\text{Fe}(\text{CN})_6]^{3-}$ solution (in PBS pH 7.0). Scan rate = 50 mVs^{-1} .

All the electrodes including the bare Pt showed the $\text{Fe}^{3+}/\text{Fe}^{2+}$ redox peaks of the $[\text{Fe}(\text{CN})_6]^{4-}/[\text{Fe}(\text{CN})_6]^{3-}$ solution. The broadness of the peaks at around 0.5 V for the Pt-CMC-Au and Pt-CMC-AuO electrodes could be due to the overlap between the ferric cyanide $\text{Fe}^{3+}/\text{Fe}^{2+}$ peak and Au^{2+}/Au

redox process. The peak current responses of the electrodes are in the sequence: Pt-CMC-AuO (127 μA) > Pt-CMC-Au (87.3 μA) > Pt-CMC (78.9 μA) > Pt-AuO = Pt-Au (25.9 μA) > Pt (18.9 μA).

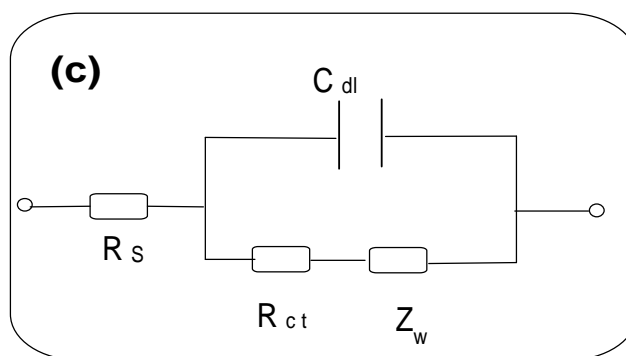
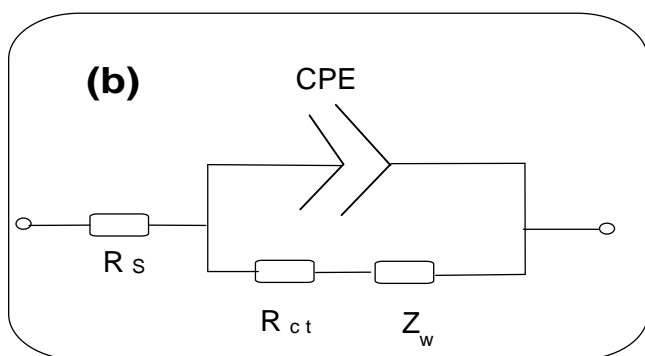
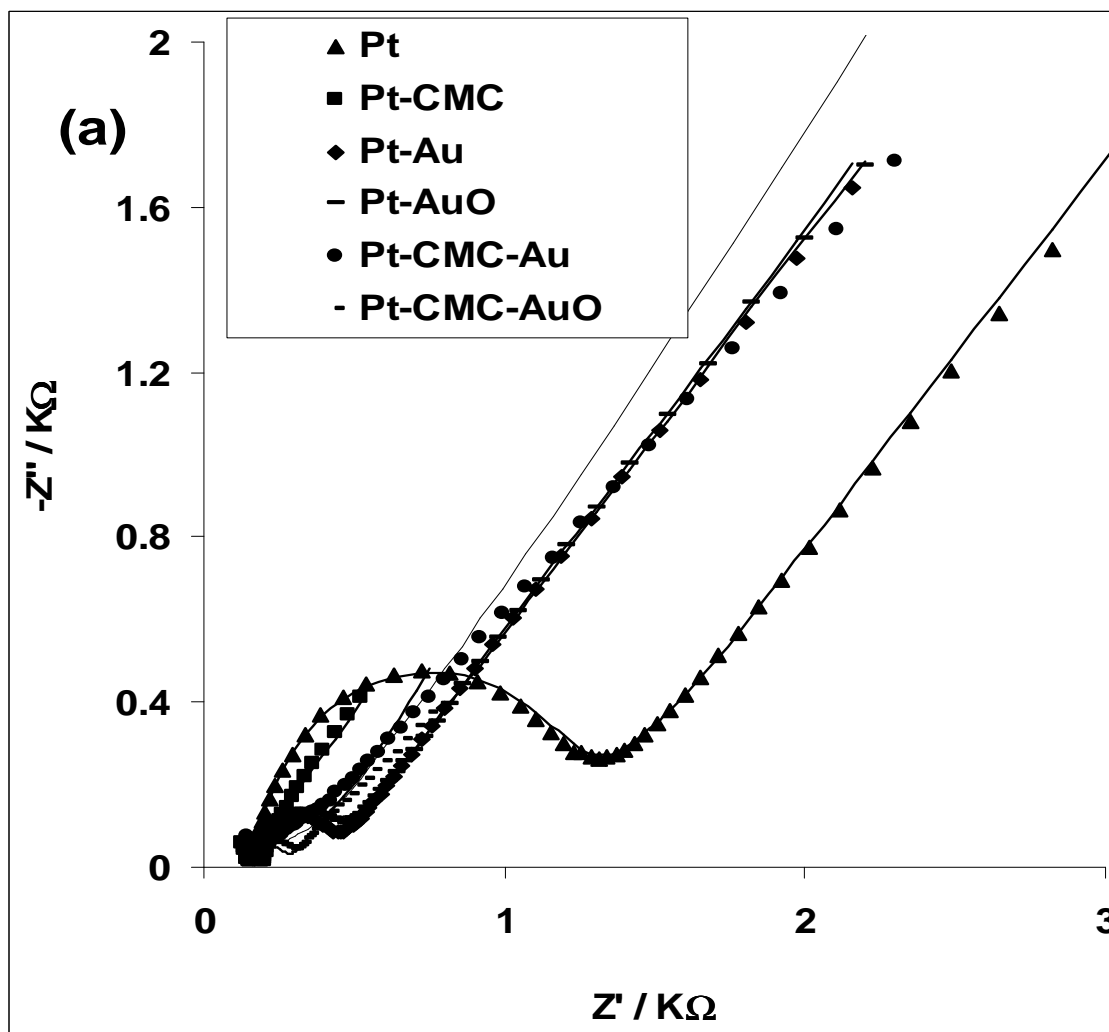


Figure 5. (a) Typical Nyquist plots obtained for some of the electrodes in 5 mM $[\text{Fe}(\text{CN})_6]^{4-} / [\text{Fe}(\text{CN})_6]^{3-}$ solution at a fixed potential of 0.2 V. The data points are experimental while the solid lines in the spectra represent non-linear squares fits. (b) and (c) represent the circuit used in the fitting of the EIS data in (a).

Electrochemical impedance spectroscopic (EIS) techniques was employed to further probe the electron transport phenomenon at the electrode-electrolyte interface [27] in 5 mM $[\text{Fe}(\text{CN})_6]^{4-}/[\text{Fe}(\text{CN})_6]^{3-}$ solution at a fixed potential of 0.2 V. Typical Nyquist plots obtained for some of the electrodes are shown in Figure 5a.

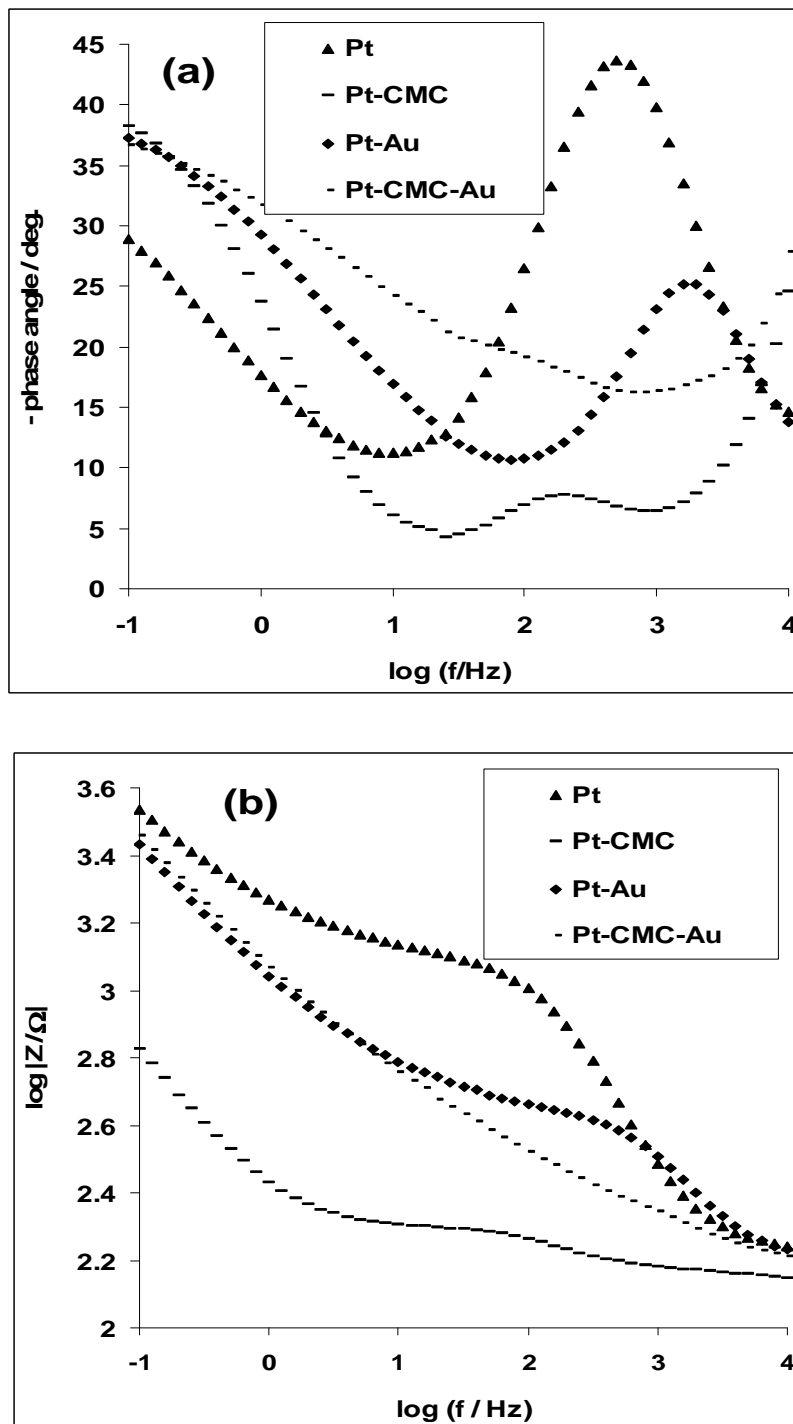


Figure 6. Is the Bode plots obtained for some of the electrodes, showing (a) the plots of -phase angle / deg. vs $\log (f / \text{Hz})$ and (b) the plot of $\log |Z / \Omega|$ vs $\log (f / \text{Hz})$.

The experimental data were successfully fitted with the Randles circuit model (Figure 5b and c) where the element R_s is the electrolyte resistance, R_{ct} is the electron transfer resistance, C_{dl} is the double-layer capacitance, CPE represents the pseudocapacitance or constant phase element, Z_w is the Warburg impedance relating to the semi-infinite linear diffusion. The parameters were fitted with satisfactory results as indicated by the percentage errors of fittings (Table 1).

Table 1. Impedance data obtained for the Pt modified electrodes in 5 mM $Fe(CN)_6^{4-}/[Fe(CN)_6]^{3-}$ solution at 0.2 V (vs Ag|AgCl sat'd KCl). All values were obtained from the fitted impedance spectra after several iterations of the circuits used. The values in parentheses are percentage errors of data fitting.

Electrode	Impedance Data				
	$R_s / \Omega cm^2$	$CPE / \mu F cm^{-2}$	N	$R_{ct} / \Omega cm^2$	$Z_w / m\Omega$
Pt	4.04 (0.03)	14.0 (5.39)	0.87 (0.75)	26.95 (0.02)	0.52 (1.27)
Pt-CMC	1.61 (0.66)	720.0 (14.23)	0.55 (3.30)	2.44 (0.41)	0.16 (36.17)
Pt-Au	3.82 (0.02)	10.8 (6.23)	0.90 (0.92)	6.82 (0.02)	0.52 (0.38)
Pt-AuO	2.89 (0.20)	2.0 (28.15)	0.68 (6.43)	9.08 (0.17)	0.52 (2.05)
Pt-CMC-Au	3.40 (0.16)	25.6 (18.26)	-	3.09 (0.21)	0.42 (3.16)
Pt-CMC-AuO	3.25 (0.12)	68.8 (13.97)	-	3.43 (0.16)	1.86 (5.59)

The CMC modified electrode had better electron transport with lower R_{ct} values compared with the other electrodes (Table 1) and these results agreed with that from CV. The Bodes plots (Fig. 6a and b) show the capacitive (charge storage) or resistance to charge transfer behaviour of some of the modified electrodes. The CMC modified electrodes, Pt-CMC, Pt-CMC-AuO and Pt-CMC-Au have lower phase angles, 7.7° , 16.1° and 19.4° respectively compared with the bare Pt (43.6°) or Pt-Au (25.2°). The results further agreed with the R_{ct} values which imply there was fast charge transfer process at the CMC modified electrode. Thus, the lower the phase angle, the lower the capacitive behaviour and the higher the conductive or charge transfer properties of the sensor [28].

3.3. Voltammetric and Impedimetric studies of dopamine and epinephrine at the modified electrodes.

Figure 7 is the comparative cyclic voltammograms of (a) dopamine (DA) and (b) Epinephrine (EP) at the bare Pt and Pt modified electrodes in 0.1 M PBS (pH 7.0) containing 0.1 mM DA and EP solutions respectively. The CV evolutions of these electrodes in DA are typical for DA oxidation process where the anodic peak corresponds to oxidation of DA to dopaminoquinone (DA^+) and the cathodic peak corresponds to reduction of dopaminoquinone to leucodopaminoquinone [29]. On the other hand, the CVs evolutions in EP are typical of epinephrine redox process [28-30]. The differences observed on the CMC modified electrodes are the following: (1) A redox couple at the positive

window with anodic and cathodic peaks at about 0.2 and 0.03 V corresponding to the oxidation of epinephrine to epinephrinequinone.

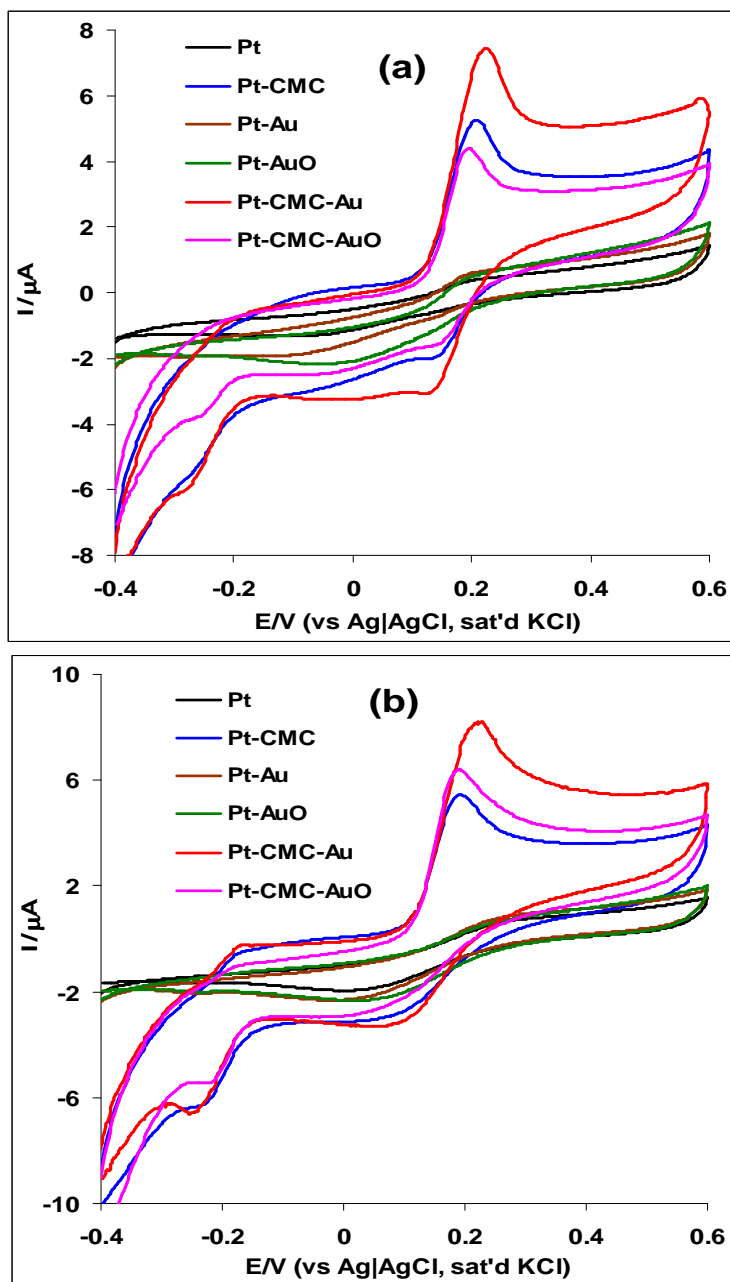


Figure 7. Comparative current response of the Pt, Pt-CMC, Pt-Au, Pt-AuO, Pt-CMC-Au and Pt-CMC-AuO in (a) 0.1 mM DA solution in pH 7.0 PBS and (b) 0.1 mM EP solution in pH 7.0 PBS, scan rate = 25 mV/s.

This is contrary to the normally irreversible peak obtained within the oxidation potential window for epinephrine [30-32]. The redox behaviour of the analyte on the CMC modified electrodes in this potential window could be due to the very stable, redox active Au^{2+}/Au catalyst mediating the oxidation process. (2) The presence of CMC amplified the second anodic peak not so well seen in the

Pt electrode only. (3) At the negative potential window, a cathodic peak ($E_{1/2} \sim -0.26$ V) corresponding to reduction of epinephrinequinone to leucoadrenochrome, and an anodic peak ($E_{1/2} \sim -0.16$ V) which corresponds to the oxidation of leucoadrenochrome to adrenochrome couple were observed on the CMC modified electrodes implying the role of CMC in improving the redox process at the electrode during electrocatalytic oxidation of epinephrine. The current response of each electrode after the buffer current subtraction follow the trend: Pt-CMC-Au (38.02 μ A) > Pt-CMC-AuO (28.22 μ A) > Pt-CMC (\sim 25.84 μ A) \gg Pt-AuO (3.03 μ A) > Pt-Au (2.26 μ A) > bare Pt (1.09 μ A) for DA; and Pt-CMC-Au (50.76 μ A) > Pt-CMC-AuO (39.45 μ A) > Pt-CMC (\sim 29.90 μ A) \gg Pt-AuO (4.28 μ A) > Pt-Au (2.98 μ A) > bare Pt (1.83 μ A) for EP. Compared with the bare Pt, the Pt-Au or Pt-AuO modified electrodes gave current response of 2 to 3 times higher (at a lower peak or formal potential) than the bare Pt electrode towards the analytes, which is expected for a chemically modified electrode. However, the electrode response was much enhanced in the presence of CMC as demonstrated by the current responses of Pt-CMC-Au and Pt-CMC-AuO, which were approximately 35 and 26 times higher in DA, 28 and 22 times higher in EP compared with bare Pt electrode. This result agreed with other reports where the enhancement of the chemical sensors was as a result of the carbon nanotubes acting as an electrical conducting nanowire between the modifier and the base electrode [11,12,14,32]. This study also demonstrated the better catalysis of DA and EP on Pt-CMC-Au electrode compared with earlier reports where the catalysis of DA was favoured on the metal oxide modified electrode [33,34]. Hence, the Pt-CMC-Au electrode was used for the remaining experiments reported in this work.

Impedimetric studies were also carried out to monitor the mechanism of the electron transfer process at the electrode-electrolyte interface during the electrocatalytic oxidation of 0.1 mM DA and EP solutions at a fixed potential of 0.2 V and frequencies between 10 kHz and 0.1 Hz. The impedance spectra (Nyquist plots) obtained for the electrodes are presented in Figures 8a and b, while Figure 8c shows the equivalent circuits used in the fitting of the impedance data. The circuit elements are already defined under section 3.2 above except for C_{films} or C_{ads} which represents the capacitance due to adsorbed intermediates on the electrode. Unlike other electrodes which are successfully fitted with circuit model RQ (RC) (Fig. 8C1), effort fitting the Pt-CMC-Au electrode with this circuit proved very difficult or impossible, with 100 % errors. Circuit RC (RC) (Fig. 8C2) gave relatively satisfactory results but with higher % error values especially for the R_{ct} data. However, the Pt-CMC-Au electrode was successfully fitted with minimum error values and reliable R_{ct} data using circuit model Q(W[RC]) (Fig. 8C3). The charge transfer resistance R_{ct} is lowest at the Pt-CMC-Au electrode ($R_{\text{ct}} = 9.1 \Omega\text{cm}^2$ in DA) and ($R_{\text{ct}} = 9.4 \Omega\text{cm}^2$ in EP) compared with bare Pt electrode (2325.0 and 3067.5 Ωcm^2 in DA and EP respectively). This finding further confirms the CV data and also indicates that the electron transfer process is faster at Pt-CMC-Au electrode during DA and EP electrooxidation than with other electrodes. This is achieved because of the presence of the CMC on the electrode. The CMC creates a porous and large surface area that mediates or favours the analyte/catalyst electrocatalytic process. It can be concluded that the rate for the oxidation of DA and EP is the same based on their R_{ct} values at the Pt-CMC-Au modified electrode. On the other hand, oxidation of the analytes at the AuO modified electrodes was poor relative to recently reported studies where Fe_2O_3 modified electrode gave better performance towards DA electrocatalytic oxidation than with Fe [33,34].

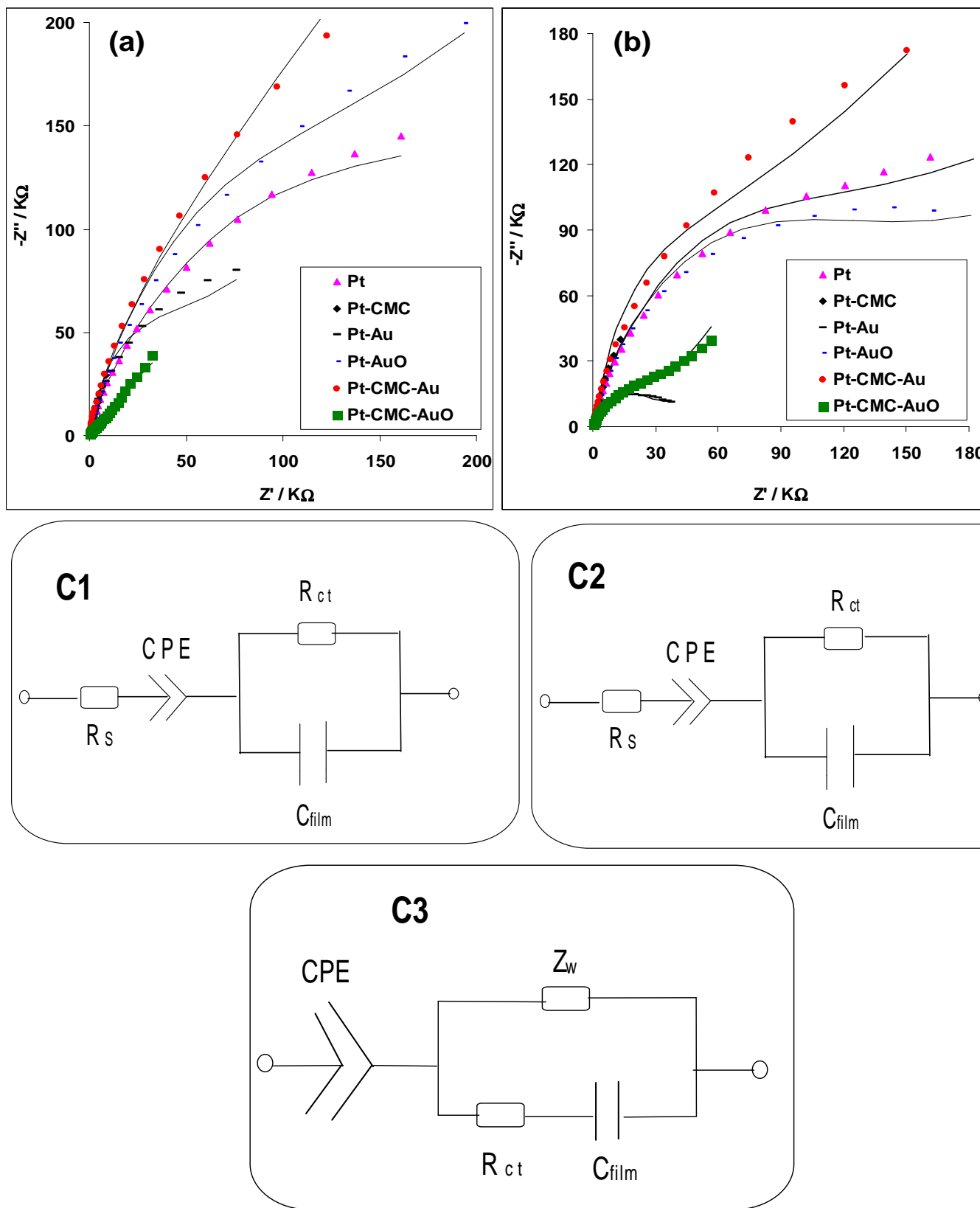


Figure 8. Typical Nyquist plots obtained for Pt-CMC-Au in (a) 0.1 mM DA solution in PBS 7.0 and (b) 0.1 mM EP solution in PBS 7.0 respectively (at fixed potential 0.2 V vs Ag|AgCl, sat'd KCl). (c) Represents the circuit used in the fitting of the EIS data in (a).

The higher C_{ads} values, 331.6 μFcm^{-2} in DA and 225.2 μFcm^{-2} in EP for the Pt-CMC-Au electrode compared with the pseudocapacitance or CPE values of the same electrode in the analytes (86.0 and 104.0 μFcm^{-2} in DA and EP respectively) suggests adsorption of oxidation intermediates leading to an increase in the charge storage properties of the electrode. Similar capacitive behaviour was reported for DA sensing using a fibre (SiC-C) electrode and according to the author, this behaviour is highly desirable for chemical and electrochemical stability of the electrode [35]

3.4. Impact of varying scan rate

Effect of scan rate (ν) was investigated by carrying out cyclic voltammetry experiments at constant concentration of 1 mM of DA and EP respectively in 0.1 M PBS using the Pt-CMC-Au electrode. From the CV (not shown), a pair of unsymmetrical redox peak at *ca* 0.2 V was observed for DA and EP. A second redox peak at about -0.16 V was also observed for EP. In both analytes, the anodic and cathodic peaks increase simultaneously with increase in scan rates (25–1000 mV s^{-1}).

From the Randles-Sevcik Equation (Eqn 1) for a reversible process [34],

$$I_p = (2.69 \times 10^5) n^{3/2} [O] A (D\nu)^{1/2} \quad (1)$$

plots of the anodic current (I_{pa}) against the square root of scan rate ($\nu^{1/2}$) (not shown) for the scan rate range studied for DA and EP gave a linear relationship with a little deviation from the zero intercept expected for a pure diffusion-controlled redox process [36]. The result suggests interplay of both diffusion process and adsorption of reaction intermediates of DA or EP at the electrode. The results agreed with other reports on oxidation of DA and EP on modified electrodes [32]. Similarly, using Tafel equation below [36]:

$$E_p = \frac{b}{2} \log \nu + \text{constant} \quad (2)$$

where the Tafel slope $b = 2.303RT/\alpha n_{\alpha}F$, R is the ideal gas constant, T is the absolute temperature, F is the Faraday constant, α is the charge transfer coefficient, n_{α} is the number of electrons involved in the rate-determining step, the plot of E_p vs. $\log \nu$ (not shown) gave slope values of 68.2 and 209.6 corresponding to a Tafel value of 136.4 and 419.2 mV dec^{-1} for the low (25-400 mVs^{-1}) and high (500-1000 mVs^{-1}) scan rate range respectively for DA electrooxidation. Using a similar plot, Tafel values of 162.8 and 554.2 mV dec^{-1} were obtained for the electrode in EP at low and high scan rates range studied. A Tafel value greater than 118 mV dec^{-1} for a one-electron process in the rate-determining step suggests adsorption of reaction intermediates on the electrode [37]. Similar results were obtained for EP on CoOCPc and MnOCPc gold modified electrode [32]. Therefore, the results obtained in this study suggest low adsorption process at low scan rate compared with high scan rate and thus, similar reaction mechanisms for DA and EP on the Pt-CMC-Au electrode.

3.5. Concentration study

Concentration study was carried out by investigating the response of Pt-CMC-Au electrode to the different concentrations of DA and EP using square wave voltammetry (SWV) experiments at a fixed potential of 0.20 V as exemplified by the voltammograms for DA in Figure 9.

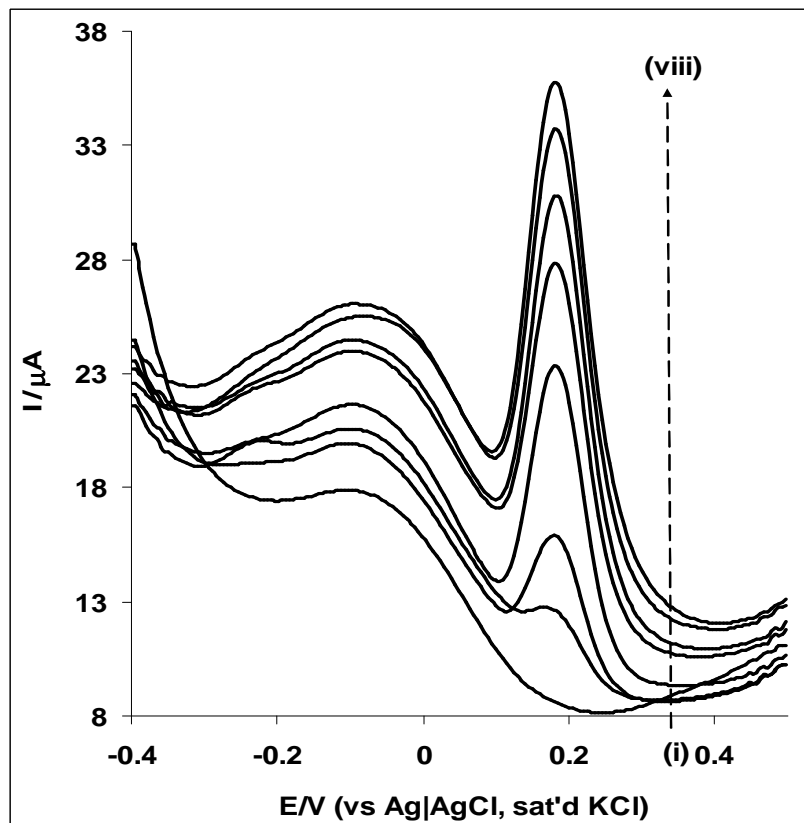


Figure 9. Typical examples of square wave voltammograms obtained for the Pt-CMC-Au in 0.1 M PBS containing different concentration of DA (0.0, 0.99, 1.96, 3.85, 4.76, 5.66, 7.41 and 9.09 μM , inner to outer).

The plot of current response against concentration (not shown) gave a linear relationship with sensitivity of $4.015 \pm 0.029 \mu\text{A}\mu\text{M}^{-1}$ for DA, and $0.615 \pm 0.010 \mu\text{A}\mu\text{M}^{-1}$ for EP respectively. The limit of detection ($\text{LoD} = 3.3 \sigma/m$ [38], where σ is the relative standard deviation of the intercept and m , the slope of the linear current versus the concentration of DA or EP) was $75 \pm 6.5 \text{ nM}$ for DA and $350 \pm 28.4 \text{ nM}$ for EP. The limit of detection obtained for DA in this study is two order of magnitude less and better compared with the $0.36 \mu\text{M}$ reported for the analyte on EPPGE-SWCNT- Fe_2O_3 [34] or $0.33 \mu\text{M}$ reported on EPPGE-MWCNT- Fe_2O_3 [33] using a similar method. The LoD for DA and EP in this study are better or compared with that obtained on other modified electrodes [32,39-43]. Since DA exists at micro molar concentrations in biological fluid [44], the nM detection of DA on Pt-CMC-Au electrode is an advantage for its application in real sample analysis.

From chronoamperometric studies and using the expression in Equation 3 [45], the catalytic rate constant (k) for the oxidation of DA and EP at the Pt-CMC-Au electrode was estimated.

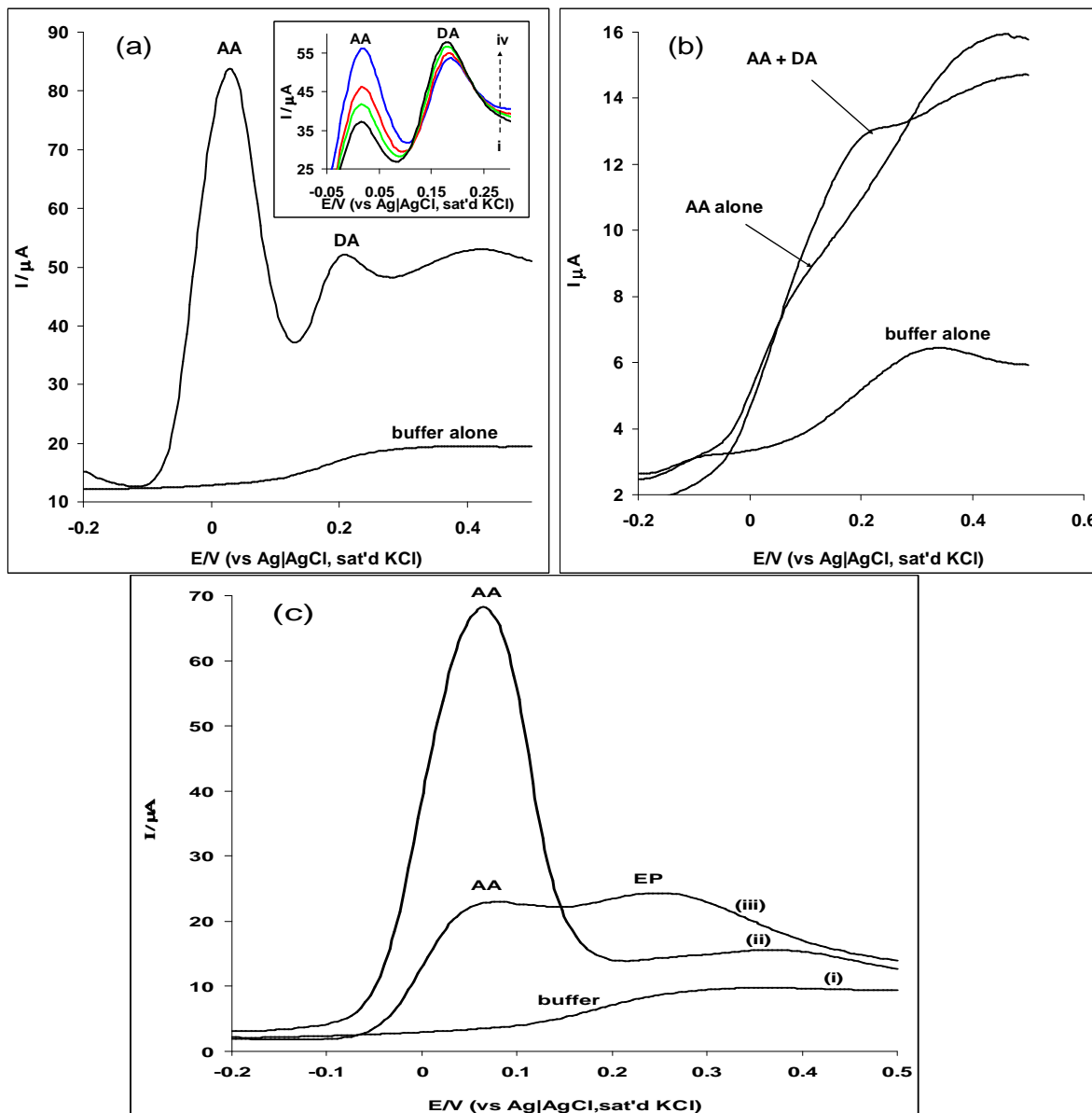


Figure 10. Typical square wave voltammogram responses of (a) Pt-CMC-Au electrode in 0.1 M pH 7.0 PBS alone and mixture of 9.1 mM AA /9.1 μM DA. Inset in 10a represents increase in DA current responses with increasing DA concentrations (50.0, 60.0, 66.7 and 71.4 μM (i-iv; inner to outer) in a mixture of AA and DA. (b) presents AA and DA unresolved signals at the bare Pt electrode (c) showed Pt-CMC-Au electrode in (i) buffer alone, (ii) 10 mM AA alone and (iii) mixture of 9.1 mM AA and 9.1 μM EP.

$$\frac{I_{cat}}{I_{buff}} = \pi^{1/2} (kCt)^{1/2} \quad (3)$$

where I_{cat} and I_{buff} are the currents in the presence and absence of DA or EP, respectively; k is the catalytic rate constant and t is the time in seconds. K was estimated from the slope of the plots of

I_{cat}/I_{buff} vs. $t^{1/2}$ at different DA or EP concentrations (not shown) as (13.8 ± 2.4) and $(18.9 \pm 4.2) \times 10^8 \text{ cm}^3 \text{ mol}^{-1} \text{ s}^{-1}$ for DA and EP respectively.

The k value for DA is three order of magnitude higher compared with $16.4 \times 10^5 \text{ cm}^3 \text{ mol}^{-1} \text{ s}^{-1}$ reported on the EPPGE-MWCNT- Fe_2O_3 electrode [33], while k value for EP is approximately a magnitude less compared with $4.5, 3.5$ and $2.1 \times 10^7 \text{ M}^{-1} \text{ s}^{-1}$ (or $10^{10} \text{ cm}^3 \text{ mol}^{-1} \text{ s}^{-1}$) reported for EP on Au-cys-FeOCPc, Au-cys-FeOCPc and Au-cys-CoOCPc electrodes respectively [32]. The difference in the K values is due to the different degrees of catalysis of the surface modified electrode.

3.6. Interference study

The electrode simultaneously detected and separated the two signals corresponding to AA and DA at a potential separation as wide as 181 mV. This is interesting since at this signal detection, AA (9.1 mM AA) is 1000 times DA concentrations (9.1 μM).

Inset in Figure 10a showed increase in DA current with increase in DA concentrations. The result indicates no detectable AA interference for every DA concentrations, and strong resistance of the Pt-CMC-Au electrode to electrode fouling phenomenon possibly due to AA or DA oxidation products. On the other hand, no signal separation for the analytes was observed on the bare Pt electrode (Fig. 10b). A good signal separation ($E = 171.2 \text{ V}$) was also noticed for the electrode in mixture of 9.1 mM AA and 9.1 μM EP (Fig. 10c). An inseparable or unresolved peak was observed for the analytes at bare Pt electrode (not shown) even with increasing EP concentrations. This study further emphasise the significance of chemically modified electrode in improving drastically its sensing behaviour towards an analyte.

4. CONCLUSIONS

This work has described the electrochemical response and the impedimetric behaviour of a CNT-gold nanoparticles decorated Pt electrode towards the detection of DA and EP. Results obtained showed that Pt-CMC-Au electrode gave the best current response and low charge transfer resistance (R_{ct}) in the analytes compared with other electrodes investigated. The impedance studies indicated that the analytes behave very similarly with relatively close charge transfer resistant values. The oxidation of the analytes was characterised with adsorption of intermediate products as indicated by their Tafel values. The molecules were detected at nano molar concentrations while the pseudocapacitive behaviour of the electrode was highly desirable for chemical and electrochemical stability. The fabricated sensor can thus conveniently separate DA and EP peaks from the interfering peak of ascorbic acid (AA).

ACKNOWLEDGEMENTS

The authors acknowledge the following institutions, University of Johannesburg (UJ) South Africa, Obafemi Awolowo University (OAU) Ile-Ife, Nigeria, and Monash University, Gippsland Campus, Churchill, Australia, for providing the research platform for this study. A.S. Adekunle is grateful to UJ for the Post Doctoral Research Fellowship.

References

1. N.Q. Jia, Z.Y. Wang, G.F. Yang, H.B. Shen, L.Z. Zhu, *Electrochem. Commun.*, 9 (2007) 233.
2. Q. Wang, N. Jiang, N. Li, *Microchemical Journal*, 68 (2001) 77.
3. F. Xu, M. Gao, L. Wang, G. Shi, W. Zhang, L. Jin, J. Jin, *Talanta*, 55 (2001) 329.
4. P. Hernandez, O. Sanchez, F. Paton, L. Hernandez, *Talanta*, 46 (1998) 985.
5. W. A. Banks, *Brain Res.*, 899 (2001) 209.
6. E.R. Peskind, R. Elrod, D.J. Dobie, M. Pascualy, E. Petrie, C. Jensen, K. Brodtkin, S. Murray, R. C. Veith, M.A. Raskind, *Neuropsychopharmacology*, 19 (1998) 465.
7. M.E.P. Hows, L. Lacroix, C. Heidbreder, A.J. Organ, A.J. Shah, *Journal of Neuroscience Methods*, 138 (2004) 123.
8. M.H. Sorouraddin, J.L. Manzoori, E. Kargarzadeh, *J. Pharm. Biomed.*, 18 (1998) 877.
9. L.Y. Zhang, S.F. Qv, Z.L. Wang, J.K. Cheng, *J. Chromatogr. B*, 792 (2003) 381.
10. H.R. Zare, N. Rajabzadeh, N. Nasirizadeh, M.M. Ardakani, *J. Electroanal. Chem.*, 589 (2006) 60.
11. B. O. Agboola, K.I. Ozoemena, T. Nyokong, T. Fukuda, N. Kobayashi, *Carbon*, 48 (2010) 763.
12. A.S. Adekunle, K.I. Ozoemena, *J. Solid State Electrochem.*, 12 (2008) 1325.
13. N. Maleki, A. Safavi, F. Tajabadi, *Anal. Chem.*, 78 (2006) 3820.
14. D. Nkosi, K. I. Ozoemena, *Electrochim. Acta*, 53 (2008) 2782.
15. Z. Song, J. Huang, B. Wu, H. Shi, J. Anzai, Q. Chen, *Sens. Actuat. B*, 115 (2006) 626.
16. J. Luo, P.N. Njoki, D. Mott, L. Wang, C.-J. Zhong, *Langmuir* 22 (2006) 2892.
17. J. Luo, P.N. Njoki, D. Mott, L. Wang, C.-J. Zhong, *Electrochem. Commun.*, 8 (2006) 581.
18. S. Senthil Kumar, J. Mathiyarasu, K.L.N. Phani, *J. Electroanal. Chem.*, 578 (2005) 95.
19. C. Retna Raj, T. Okajima, T. Ohsaka, *J. Electroanal. Chem.*, 543 (2003) 127.
20. A.-J. Wang, J.-J. Xu, Q. Zhang, H.-Y. Chen, *Talanta*, 69 (2006) 210.
21. A.I. Gopalan, K.-P. Lee, K.M. Manesh, P. Santhosh, J.H. Kim, J.S. Kang, *Talanta*, 71 (2007) 1774.
22. J. Zhang, M. Oyama, *Electrochem. Commun.*, 9 (2007) 459.
23. S. Thiagarajan, S.-M. Chen, *Talanta*, 74 (2007) 212.
24. J. A Liu, G. Rinzler, H. Dai, J.H. Hanfer, R.K. Bradley, P.J. Boul, A. Lu, T. Iverson, K. Shelimov, C.B. Huffman, F.R. Macias, Y.S. Shon, T.R. Lee, D.T. Colbert, Fullerene Pipes, *Science* 280 (1998)1253.
25. D. Giovanelli, N.S. Lawrence, S.J. Wilkins, L. Jiang, T.G.J. Jones, R.G. Compton, *Talanta*, 61 (2003) 211.
26. A.Salimi, E. Shariffi, A. Noorbakhsh, S. Soltanian, *Electrochem. Commun.*, 8 (2006)1499.
27. I.D. Raistrick, D. R. Franceschetti, J. R. Macdonald, In: Impedance Spectroscopy: Theory Experiment, and Applications, 2nd ed, E. Barsoukov and J.R. Macdonald (eds.), Wiley, Hoboken, New Jersey, 2005, Chap. 2, pp.27-128.
28. O.A. Arotiba, P.G. Baker, B.B. Mamba, E.I. Iwuoha, *Int. J. Electrochem. Sci.*, 6 (2011) 664.
29. S. Shahrokhian, S. Bozorgzadeh, *Electrochimica Acta* 51 (2006) 4271.
30. Z. Yang, G. Hu, X. Chen, J. Zhao, G. Zhao, *Colloids Surf. B: Biointerf.*, 54 (2007) 230.
31. M.D. Hawley, S.V. Tatawawadi, S. Piekarski, R.N. Adams, *J. Am. Chem. Soc.*, 89 (1967) 447.
32. B.O. Agboola, K.I. Ozoemena, *Electroanalysis*, DOI: 10.1002/elan.200804240

33. A.S. Adekunle, K.I. Ozoemena, *Int. J. Electrochem. Sci.*, 5 (2010) 1726.
34. A.S. Adekunle, B.O. Agboola, J. Pillay, K.I. Ozoemena, *Sens. Actuator: Chemical B*, 148 (2010) 93.
35. S. Singh, R.C. Buchanan, *Mat. Sc. Engnr. C.*, 27 (2007) 551.
36. A.J. Bard, L.R. Faulkner, *Electrochemical Methods: Fundamentals and Applications*, 2nd ed., John Wiley & Sons, Hoboken, NJ., 2001.
37. J.N. Soderberg, A.C. Co, A.H.C. Sirk, V.I. Birss, *J. Phys. Chem. B*, 110 (2006) 10401.
38. G.D. Christian, *Analytical Chemistry*, 6th ed. John Wiley and Sons New York, 2004, p113.
39. S. Shahrokhian, H. R. Zare-Mehrjardi, *Sens. Actuators B Chem.*, 121 (2007) 530.
40. B.N. Chandrashekar¹, B.E. Kumara Swamy, M. Pandurangachar, S.S Shankar¹, O. Gilbert¹, J.G. Manjunatha, B.S., Sherigara, *Int. J. Electrochem. Sci.*, 5 (2010) 578.
41. Ali A. Ensafi, M. Taei, T. Khayamian, *Int. J. Electrochem. Sci.*, 5 (2010) 116.
42. M. A. Fotopoulou, P. C. Loannou, *Anal. Chim. Acta*, 462 (2002), 179.
43. W. Ren, H. Q. Luo, N. B. Li, *Biosens. Bioelectron.*, 21 (2006) 1086.
44. T. Selvaraju, R. Ramaraj, *J. Electroanal. Chem.*, 585 (2005)290.
45. Z. Galus, *Fundamentals of Electrochemical Analysis*, Ellis Horwood Press, New York, 1976, p. 313, Ch. 10.